Electronic Supplementary Material (ESI) for Soft Matter.

Supporting Information for

Porous films by the self-assembly of inorganic rod-coil block copolymers. Mechanistic insights into the vesicle-to-pore morphological evolution.

Silvia Suárez-Suárez, Gabino A. Carriedo, and Alejandro Presa Soto*

†Facultad de Química. Departamento de Química Orgánica e Inorgánica. IUQOEM. Universidad de Oviedo. Julián Clavería s/n, 33006, Oviedo (Spain)

**presaalejandro@uniovi.es*

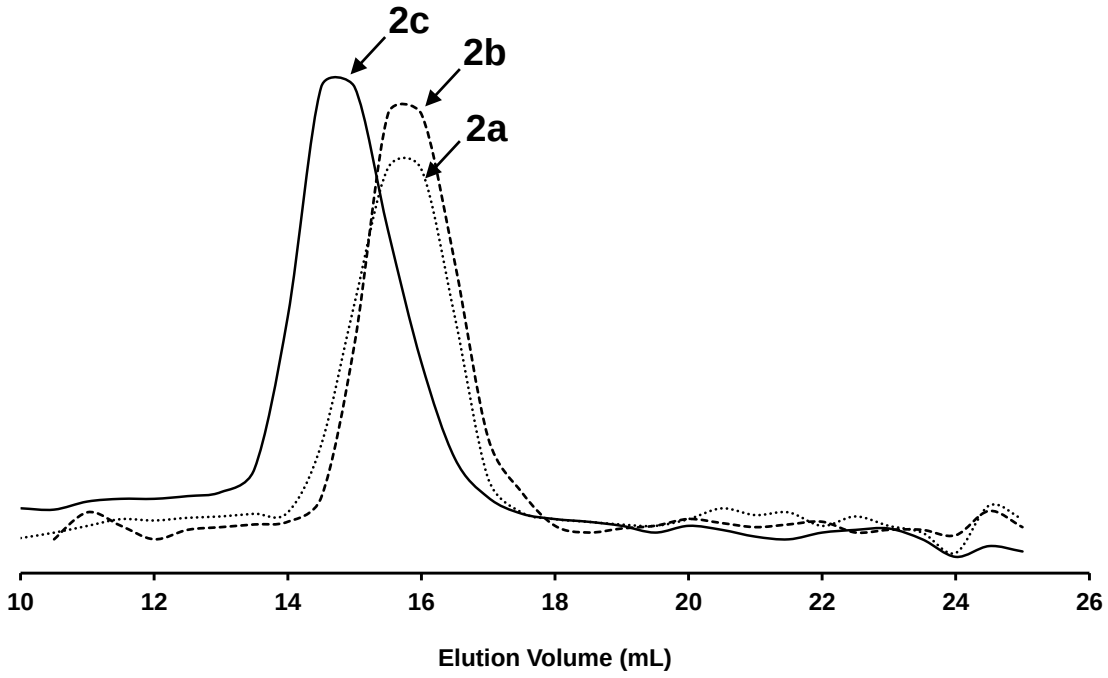

Figure S1. GPC traces of block copolymers **2a-c** using THF having tetra-*n*-butylammonium bromide (0.1 % w/w) as eluent.

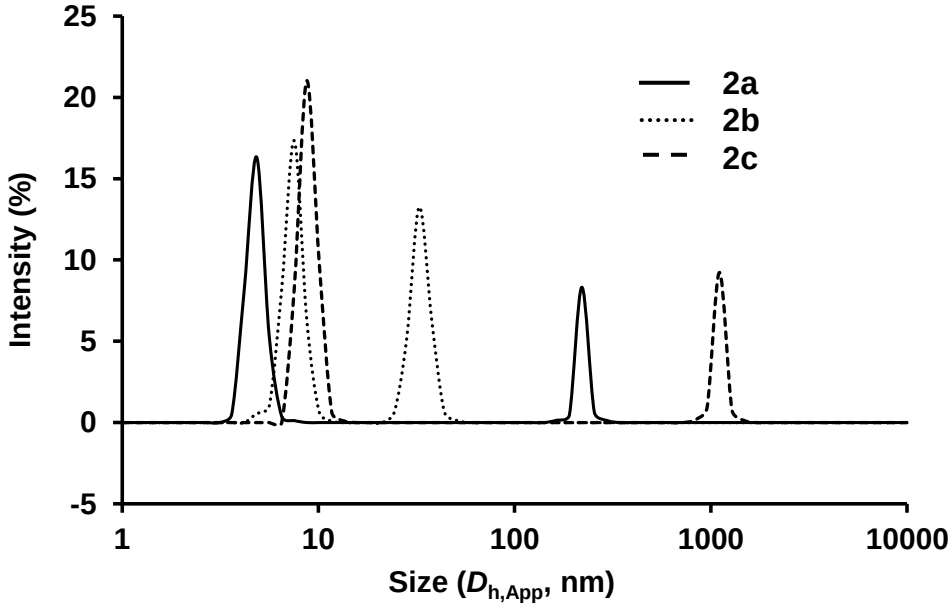

Figure S2. Dynamic light scattering traces of THF solutions (5 mg / mL) of BCPs **2a-c**.

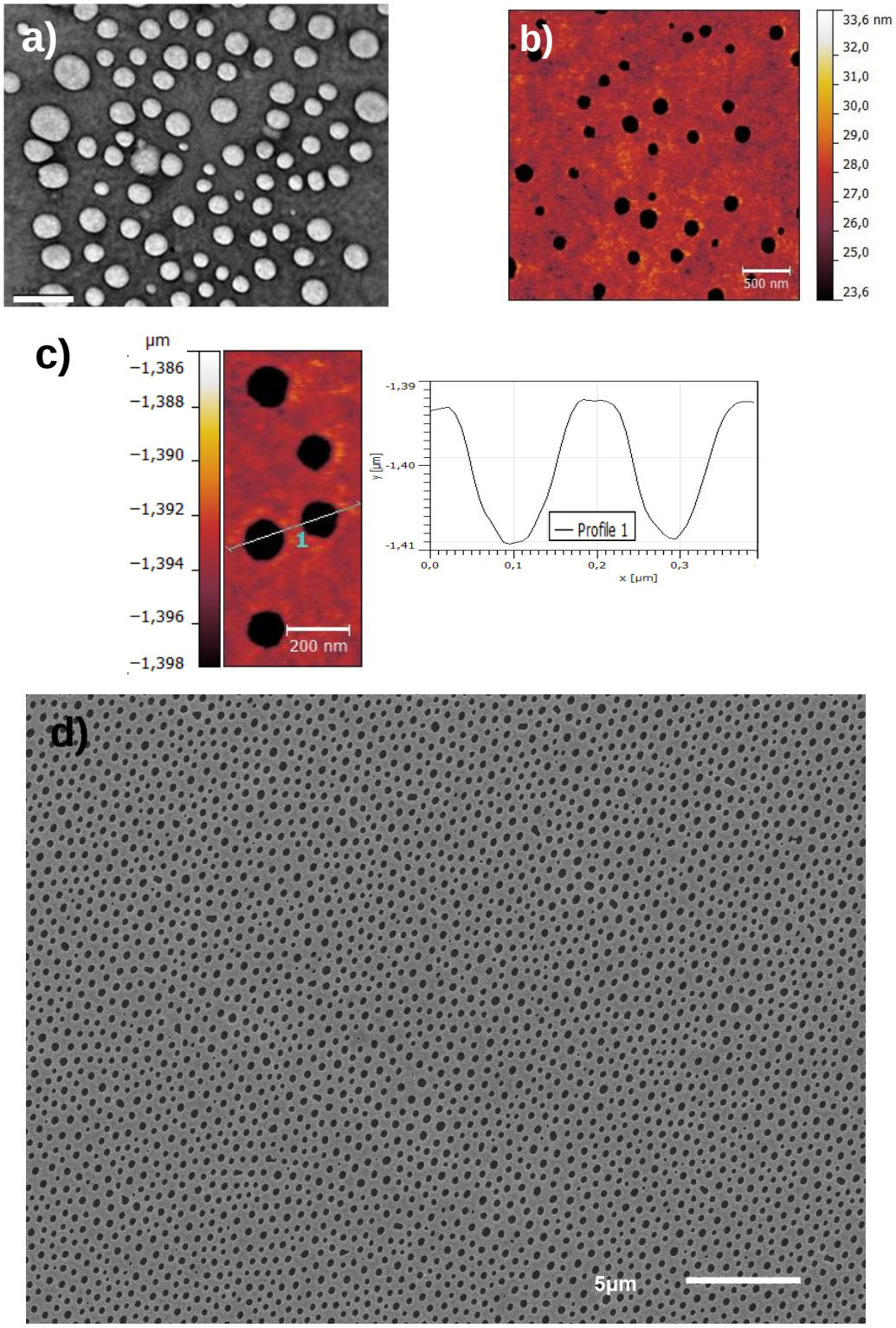

Figure S3. Porous films of BCP **2a**: a) Bright-field TEM image (inset scale bar corresponds to 500 nm). b) AFM height image. c) AFM height image (inset scale bar corresponds to 200 nm) and cross-sectional height profiles across two pores. (d) SEM image (inset scale bar corresponds to 5000 nm).

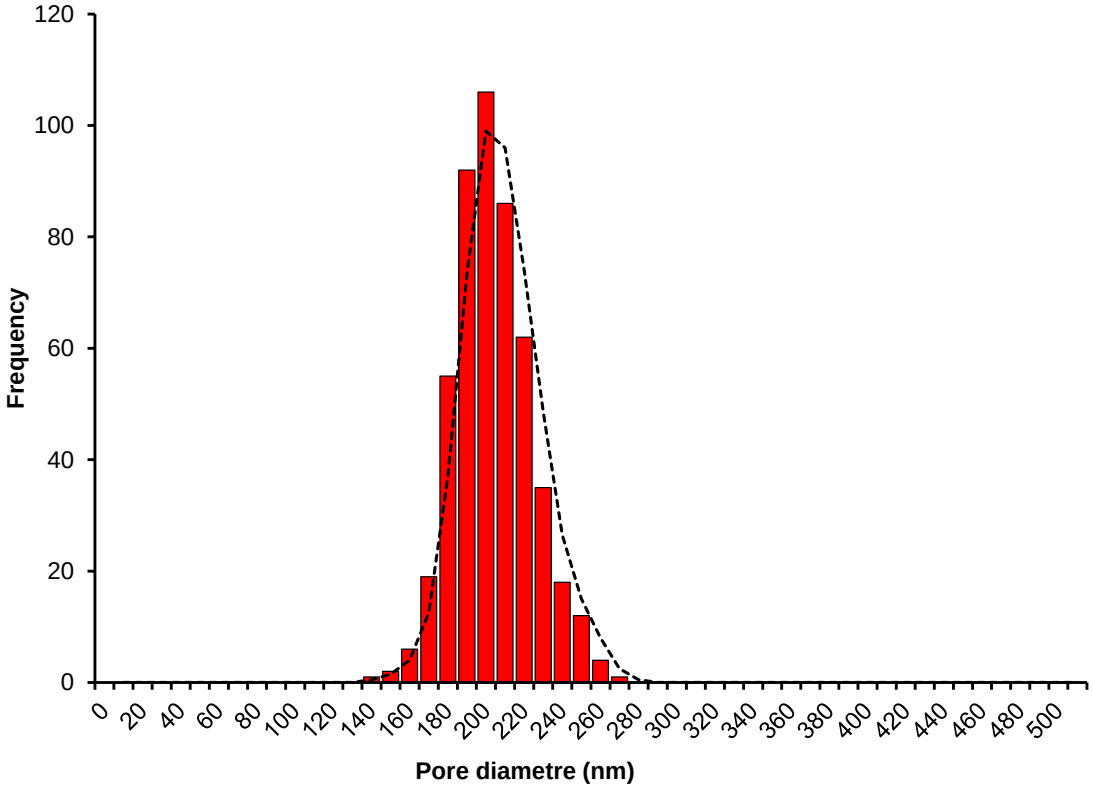

Figure S4. Histogram of the size (diameter) distribution of pores of BCP **2a** (number of objects, N = 500).

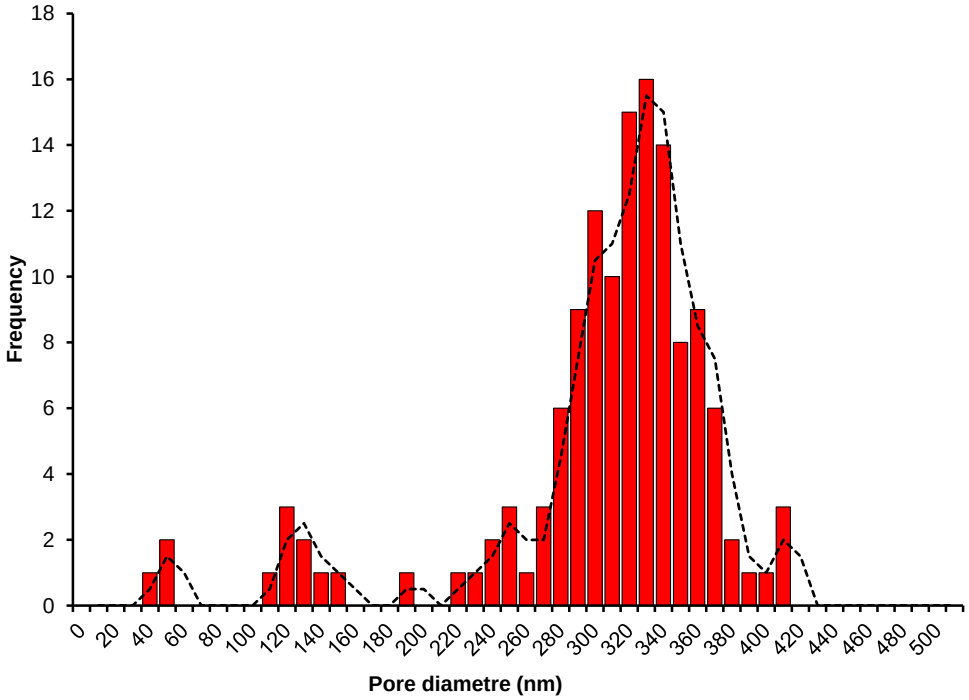

Figure S5. Histogram of the size (diameter) distribution of vesicles of BCP **2a** (number of objects, *N* = 135).

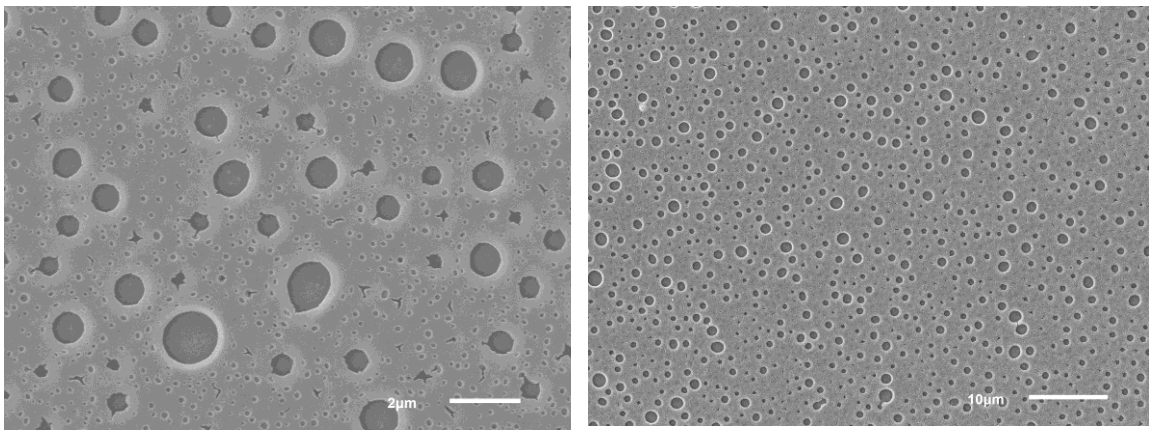

Figure S6. SEM images of porous films prepared by drop-casting of a 5 mg / mL solution of BCP **2a** in THF.

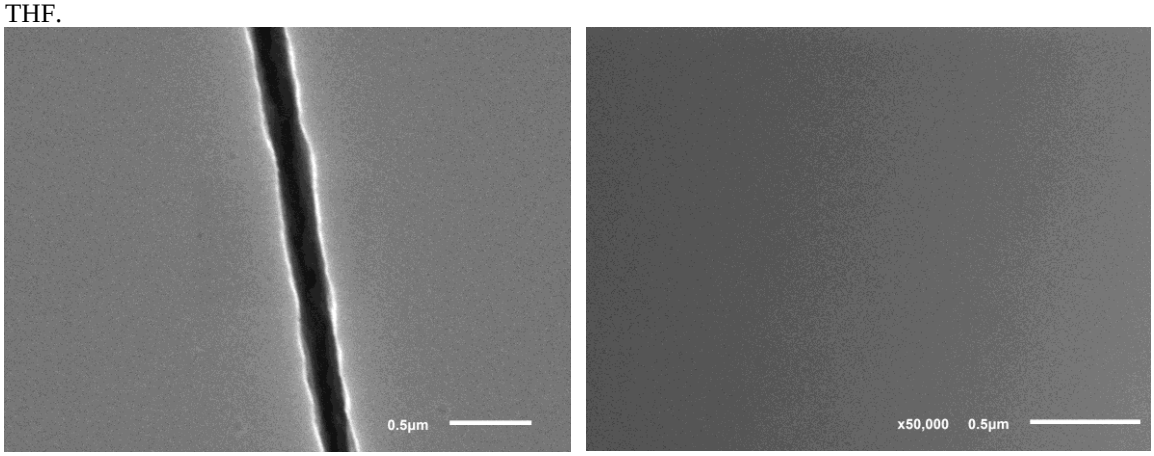

Figure S7. SEM images of porous films prepared by drop-casting of a 20 mg / mL solution of BCP **2a** in THF.

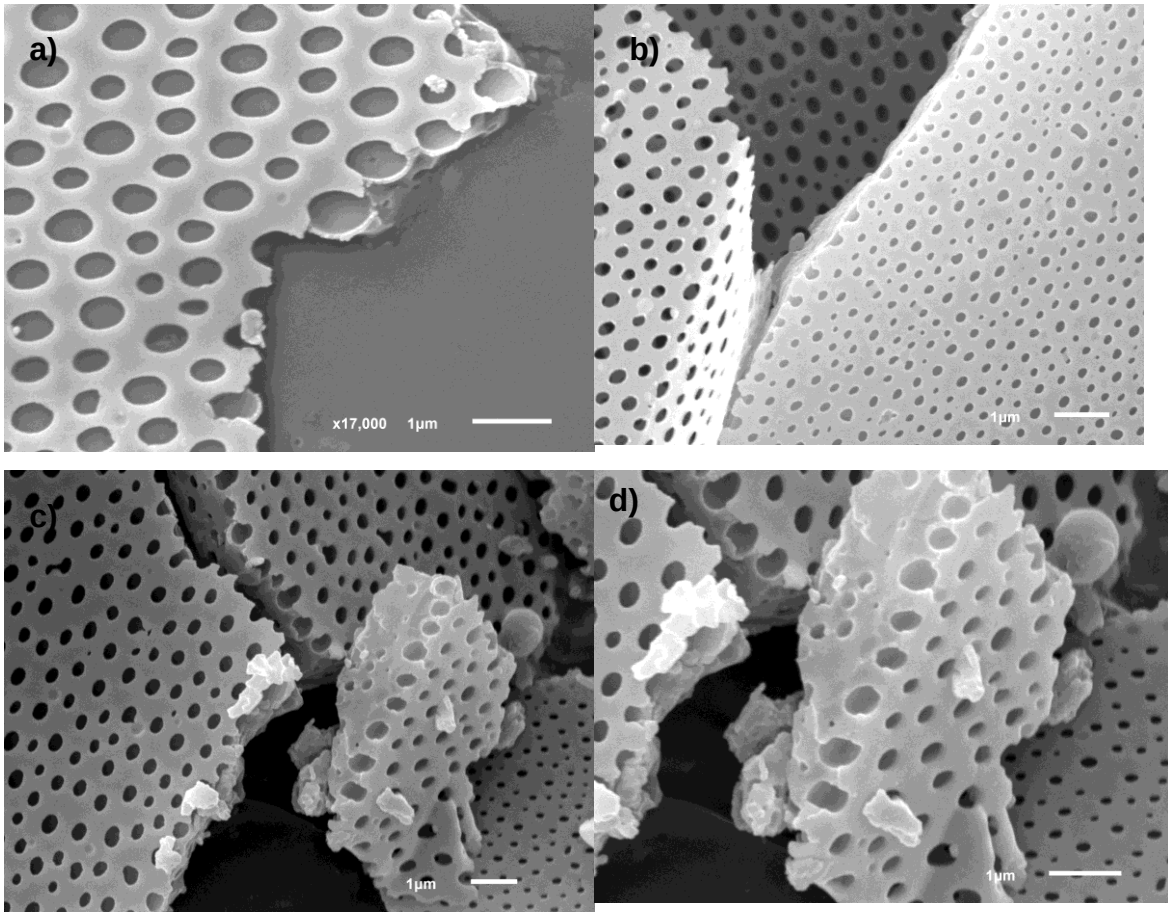

Figure S8. SEM pictures showing the structure of the pores located underneath the top-surface layer of the film of **2a**. In picture b) a flexible porous sheet can be observed at the left part of the SEM image.

at 1000 rpm

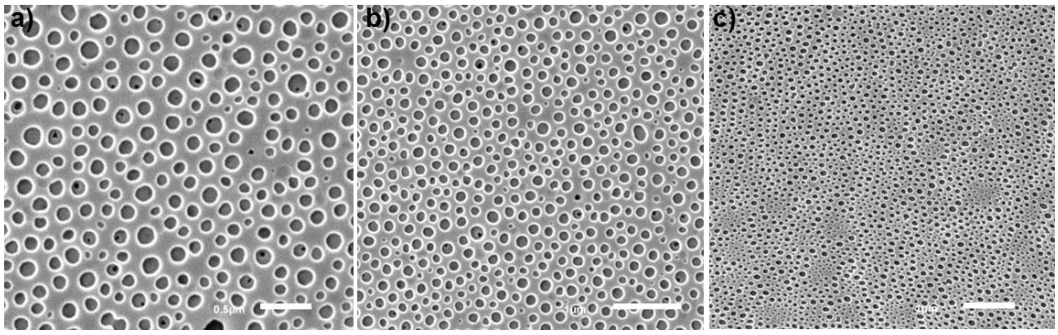

at 3000 rpm

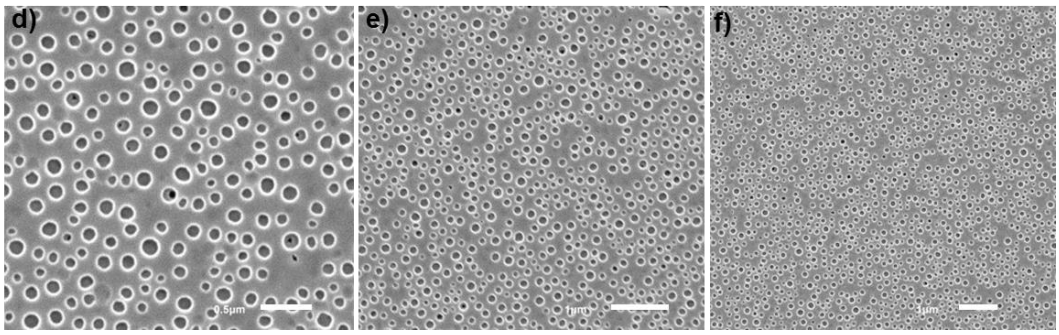

at 5000 rpm

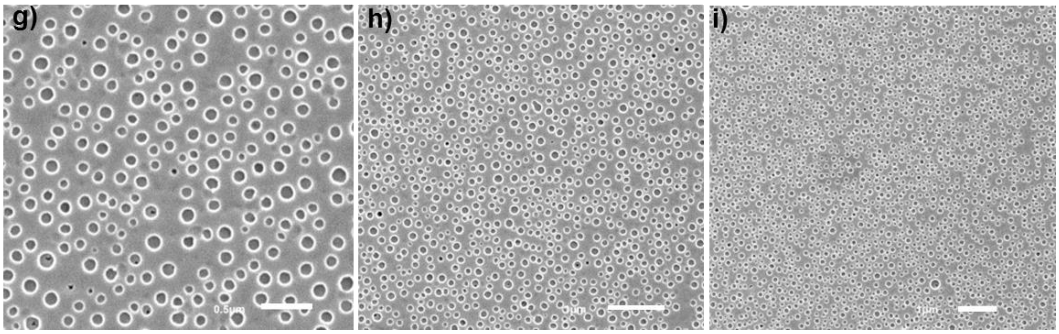

Figure S9. SEM images of porous films formed by spin-coating of a BCP **2a** solution (10 mg mL^{-1} in THF) at different rotational speeds: (a, b, c) at 1000 rpm (inset scale bars correspond to 0.5, 1 and 1 μm respectively); (d, e, f) at 3000 rpm (inset scale bars represent 0.5, 1 and 1 μm respectively); (g, h, i) at 5000 rpm (inset scale bars correspond to 0.5, 1 and 1 μm respectively).

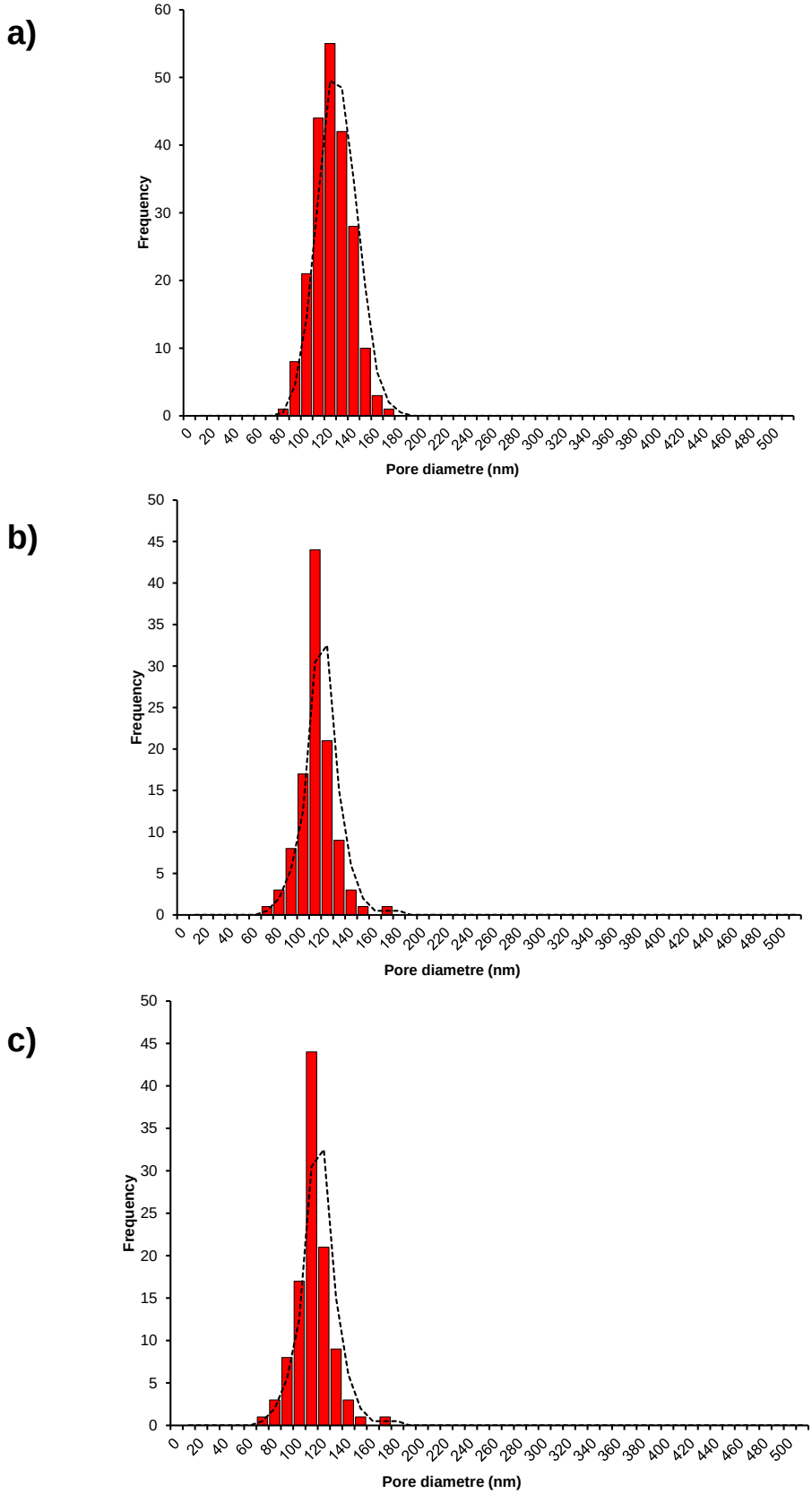

Figure S10. Histogram of the size (diameter) distribution of pores prepared by spin-coating of a 10 mg / mL solution of BCP **2a** in THF at: (a) 1000 rpm (number of objects, *N* = 213). (b) 3000 rpm (number of objects, *N* = 108). (c) 5000 rpm (number of objects, *N* = 156)

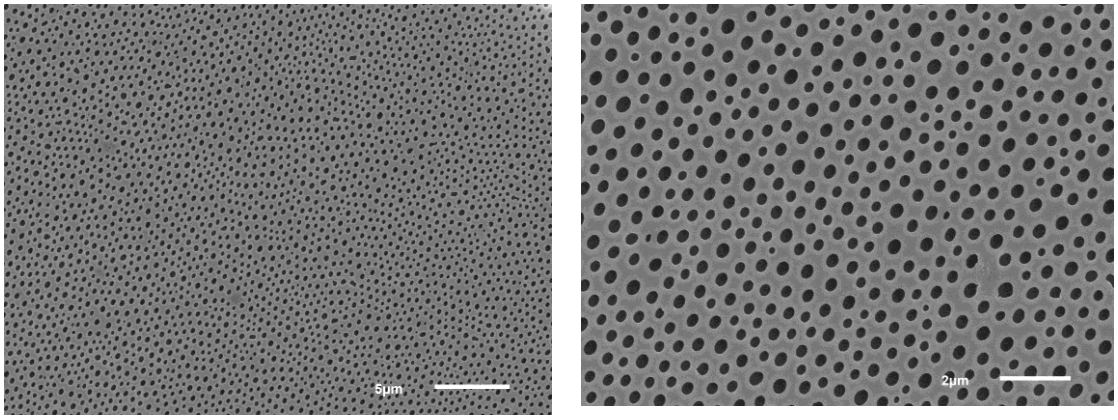

Figure S11. SEM images of the porous films of BCP **2a** after heating at 100º C during 8 hours under vacuum.

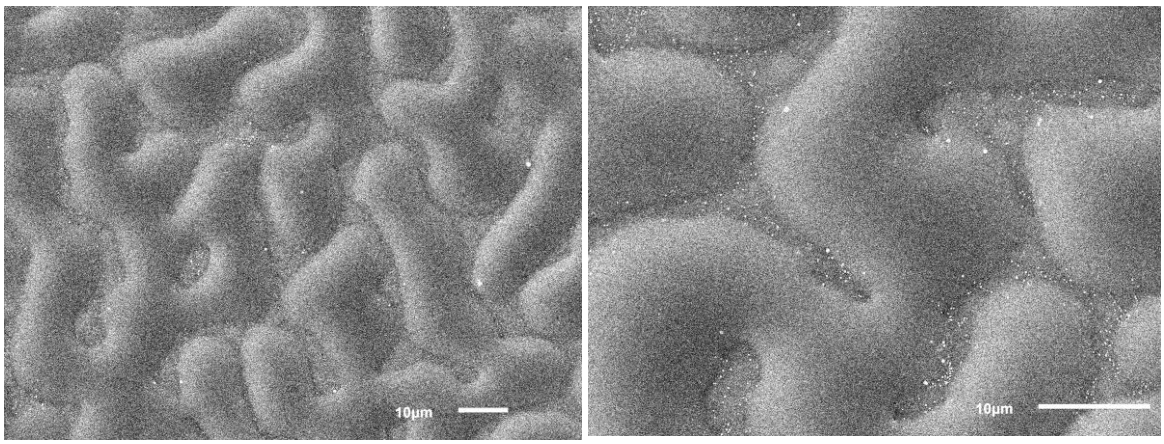

Figure S12. SEM images of the porous films of BCP **2a** after heating at 190º C during 8 hours under vacuum.

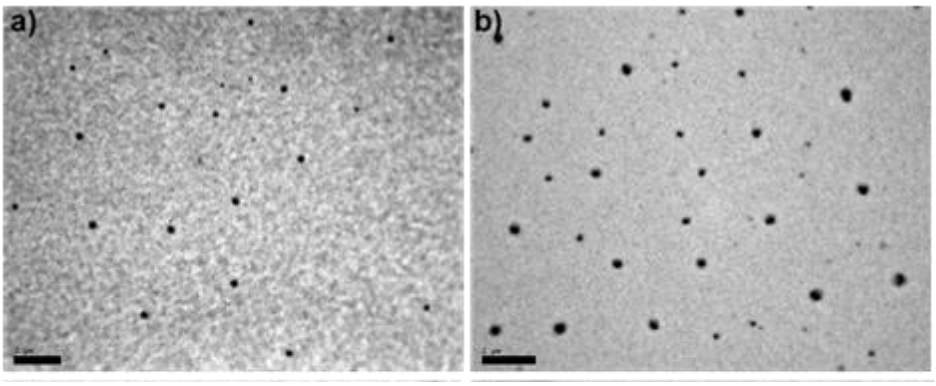

Figure S13. Bright field TEM micrographs of spherical micelles after the THF annealing (10 days). Inset scale bars correspond to 2 µm (a) and 1 µm (b).

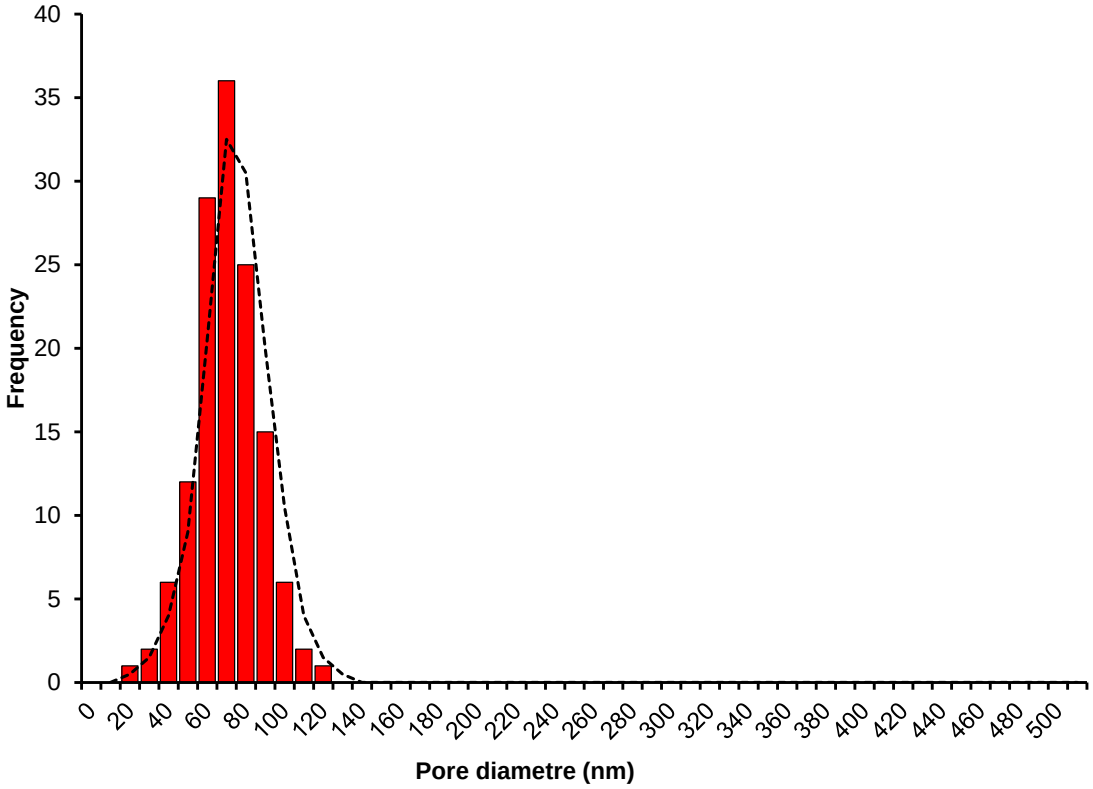

Figure S14. Histogram of the size (diameter) distribution of nanospheres of BCP **2a** (number of objects, *N* = 135) obtained after a solvent annealing (10 days) of previously formed porous films.

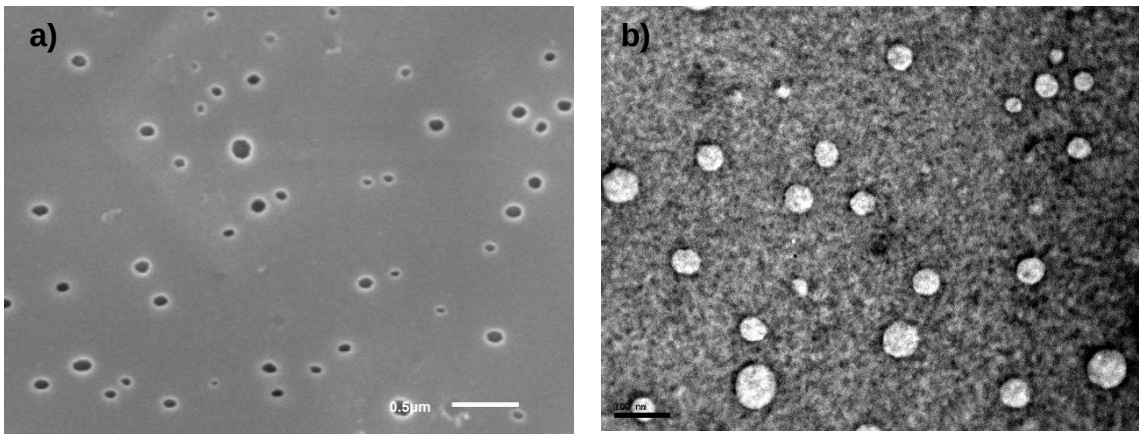

Figure S15. SEM (a) and bright TEM (b) pictures of porous films of BCP **2b** (THF, 10 mg /mL b. Inset scale bar corresponds to 200 nm)).

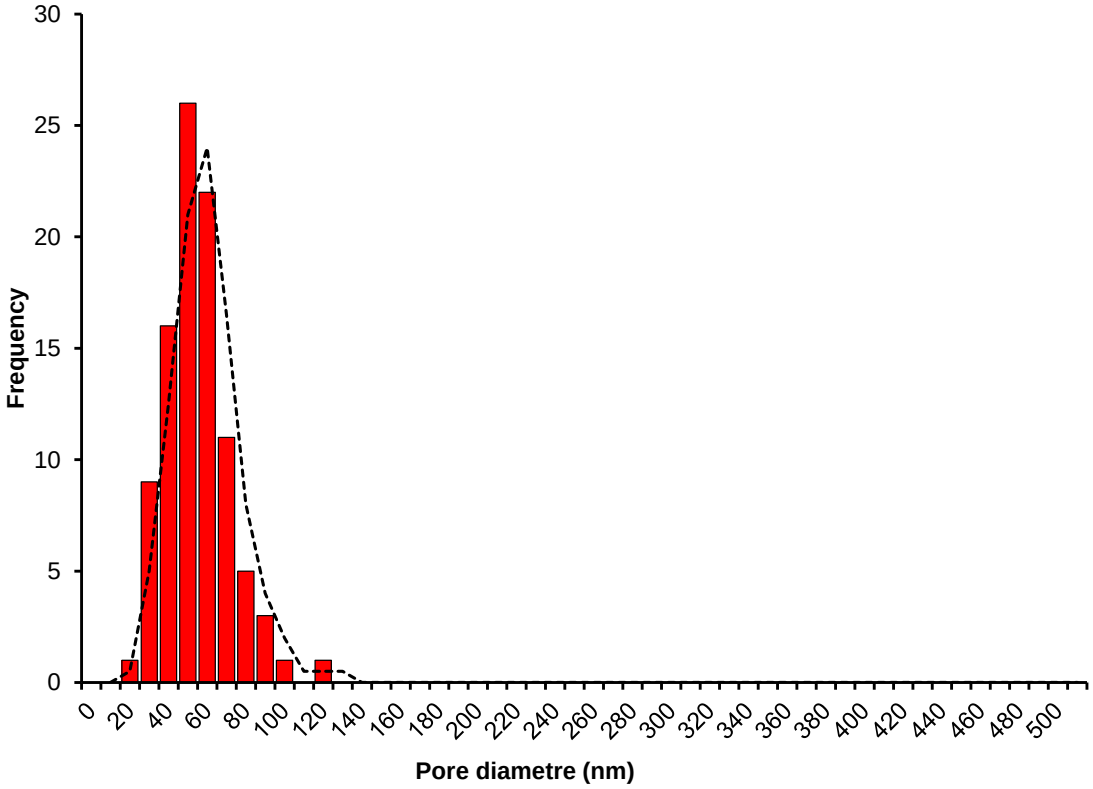

Figure S16. Histogram of the size (diameter) distribution of pores of BCP **2b** (number of objects, *N* = 95).

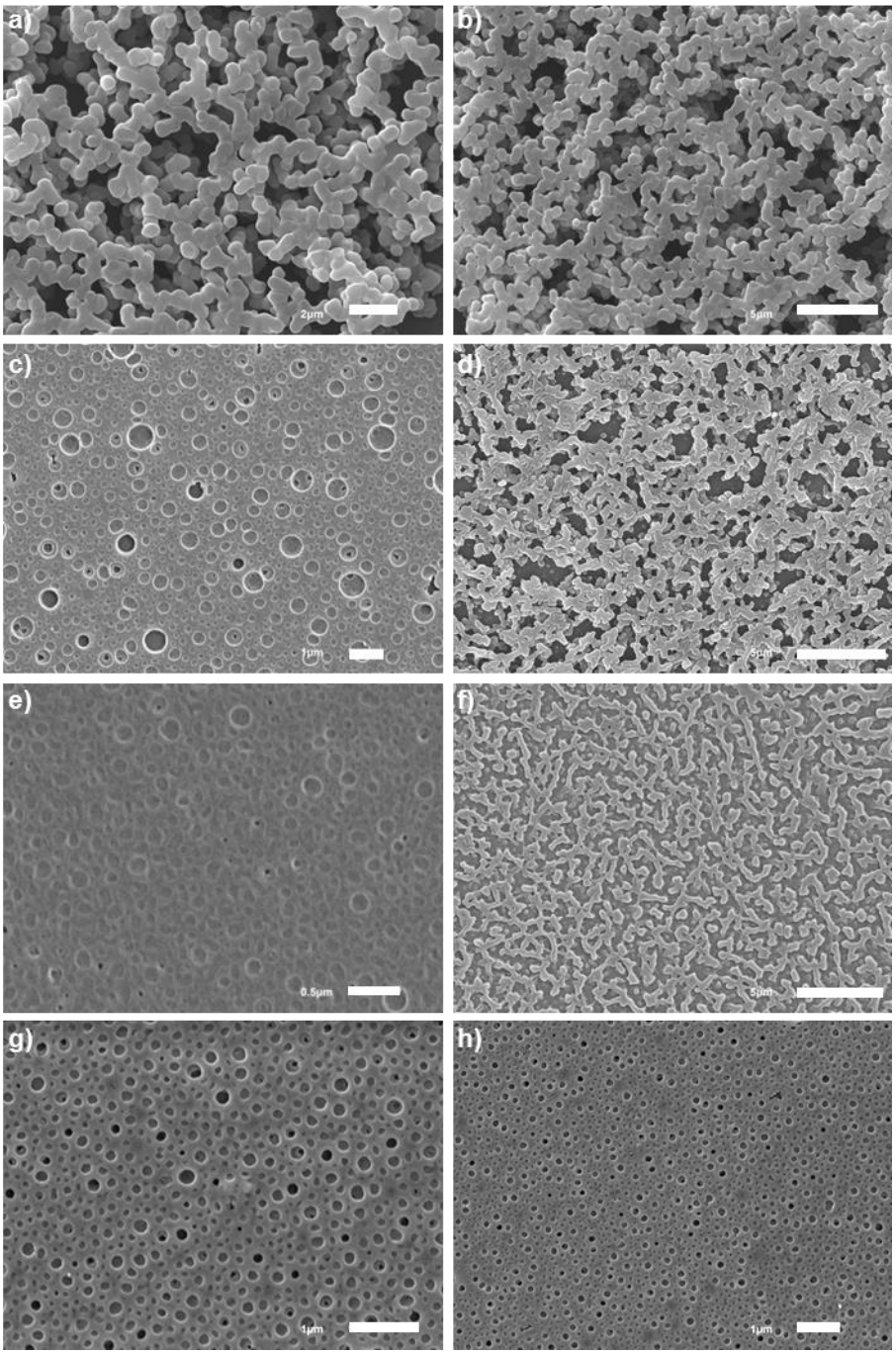

Figure S17. SEM images of porous films prepared by spin-coating of a BCP **2c** solution (10 mg mL^{-1} in THF) at different rotational speeds: (a, b) at 500 rpm (inset scale bars correspond to 2 and 5 µm respectively); (c, d) at 1000 rpm (inset scale bars represent 1 and 5 µm respectively); (e, f) at 3000 rpm (inset scale bars correspond to 0.5 and 5 µm respectively); at 5000 rpm (inset scale bars correspond to 1 and 5 µm respectively).